

Generalization of the Nyquist robust stability margin and its application to systems with real affine parametric uncertainties

Charles T. Baab¹, Juan C. Cockburn², Haniph A. Latchman³ and
Oscar D. Crisalle^{1,*†}

¹ *Department of Chemical Engineering, University of Florida, Gainesville, FL 32611, U.S.A*

² *Department of Electrical Engineering, Florida A&M University-Florida State University, Tallahassee, FL 32310, U.S.A*

³ *Department of Electrical Engineering, University of Florida, Gainesville, FL 32611 U.S.A*

SUMMARY

The critical direction theory for analysing the robust stability of uncertain feedback systems is generalized to include the case of non-convex critical value sets, hence making the approach applicable for a much larger class of relevant systems. A redefinition of the critical perturbation radius is introduced, leading to the formulation of a Nyquist robust stability measure that preserves all the properties of the previous theory. The generalized theory is applied to the case of rational systems with an affine uncertainty structure where the uncertain parameters belong to a real rectangular polytope. Necessary and sufficient conditions for robust stability are developed in terms of the feasibility of a tractable linear-equality problem subject to a set of linear inequalities, leading ultimately to a computable Nyquist robust stability margin. A systematic and numerically tractable algorithm is proposed for computing the critical perturbation radius needed for the calculation of the stability margin, and the approach is illustrated via examples. Copyright © 2001 John Wiley & Sons, Ltd.

1. INTRODUCTION

The critical-direction theory developed by Latchman and Crisalle [1] and Latchman *et al.* [2] addresses the problem of robust stability of systems affected by uncertainties that can be characterized in terms of frequency-domain value sets. The approach introduces the *Nyquist robust stability margin* $k_N(\omega)$ as a scalar measure of robustness analogous to the structured singular value μ [3] and the multivariable stability margin k_m [4]. This paper extends the critical direction theory to the more general case where the *critical value-set* may be non-convex. The key to extending the theory is the introduction of a generalized definition of the critical perturbation radius in a fashion that preserves all previous results. Non-convexity of the critical value set is observed in a number of interesting problems, including the case studied by Fu [5]

*Correspondence to: Oscar D. Crisalle, Department of Chemical Engineering, University of Florida, Gainesville, FL 32611, U.S.A.

†E-mail: crisalle@che.ufl.edu

Contract/grant sponsor: National Science Foundation; contract/grant number: CTS 9502936

consisting of rational systems where the uncertainty appears affinely in the form of real parameters that belong to a known rectangular polytope. The generalized critical direction theory is applied to this particular class of uncertain systems, and is used to calculate the required Nyquist robust margin with high precision and in the context of a computationally manageable framework.

The robust stability problem studied by Fu is part of an extensive literature on systems where the uncertainty appears in the form of parameters that vary in prescribed real intervals, a situation of relevance to many engineering problems. Early advances in this field are due to Kharitonov [6, 7] who derived necessary and sufficient conditions for the robust stability of interval polynomials, that is, polynomials with independent coefficients that take values in closed real intervals. An extension of Kharitonov's theorem to rational interval plants is proposed in Chapellat *et al.* [8], where the objective is to assess the stability of a family of plants by testing a subset of extreme plants or extreme segments. The number of extreme plants required to determine robust stability depends on the functional relationship between the uncertain parameters and their bounding interval-sets. Comprehensive results based on extreme plants or segments are known to exist only for a restricted set of uncertainty structures. A detailed account of Karitonov-like methods can be found in Barmish [9] and in the references therein. For contextual value, it is worth mentioning that many of the methods proposed are based on determining the stability of a set of Kharitonov plants (or extreme plants) derived from the interval bounding-set description. For example, Chapellat *et al.* [8] and Bartlett *et al.* [10] give conditions that use 32 Kharitonov segments or edges. Barmish [11] prove that when using first-order compensators it is necessary and sufficient that 16 of the extreme plants be stable; furthermore, under certain conditions only eight or twelve plants are necessary.

In this paper the generalized critical direction theory is applied to systems with affine parametric uncertainty and exploits earlier results of Fu [5] regarding the mapping of the uncertain parameters from their polytopic domain to the Nyquist plane to develop a computationally tractable algorithm for calculating the Nyquist robust stability margin.

The paper is organized as follows. Section 2 generalizes the critical direction theory for systems with non-convex critical value sets. Sections 3–6 are concerned with the application of the generalized theory to the case of affine uncertain rational systems with real polytopic parametric uncertainties. Section 3 introduces a precise definition of the uncertain system considered, and Section 4 derives two robust-stability theorems for these types of systems. Section 5 presents a systematic method for calculating the critical perturbation radius, and Section 6 provides two examples of the analysis method, including the case of a convex and the case of nonconvex critical value set. Overall conclusions are given in Section 7.

2. GENERALIZATION OF THE CRITICAL DIRECTION THEORY

2.1. Preliminaries

Consider the single-input–single-output linear time-invariant system

$$g(s) = g_0(s) + \delta(s) \quad (1)$$

where $g_0(s)$ is a known *nominal transfer function*, and $\delta(s) \in \Delta$ is an *unknown perturbation* belonging to a known perturbation family Δ . The focus of this analysis is on the robust stability

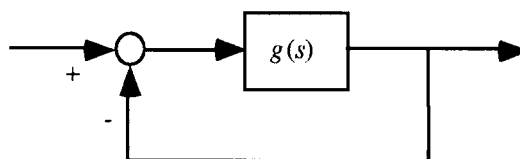


Figure 1. Unity feedback control scheme for an uncertain plant $g(s)$.

of the closed-loop system that results when the uncertain system (1) is configured in the unity negative feedback control structure shown in Figure 1. The following standard assumptions are made throughout this paper:

(A1) The nominal transfer function $g_0(s)$ is stable under unity negative feedback.

(A2) The set of allowable perturbations Δ is such that $g(s)$ and $g_0(s)$ have the same number of open-loop unstable poles.

The robust stability analysis is based on a frequency-domain description of the uncertain perturbations using value sets. The *uncertainty value set of $g(s)$ at frequency ω* is defined as

$$\mathcal{V}(\omega) := \{g(j\omega) | g(j\omega) = g_0(j\omega) + \delta(j\omega), \delta(s) \in \Delta\}$$

and $\mathcal{V}(\omega)$ is said to lie on the *Nyquist plane*. A generic uncertainty value set is shown in Figure 2.

The *critical-direction theory* advanced in Latchman and Crisalle [1] and in Latchman *et al.* [2] is based on the observation that the destabilizing perturbations occur along the *critical direction*

$$d_c(j\omega) := -\frac{1 + g_0(j\omega)}{|1 + g_0(j\omega)|}$$

which is interpreted as the unit vector with origin at the nominal point $g_0(j\omega)$ and pointing towards the critical point $-1 + j0$ (*cf.* Figure 2). This direction in turn defines the *critical line* $r(\omega) := g_0(j\omega) + \alpha d_c(j\omega)$, $\alpha \in R^+$, where R^+ denotes the non-negative real numbers. The critical line $r(\omega)$ is interpreted as a ray that originates at the nominal point $g_0(j\omega)$ and passes through the *critical point* $-1 + j0$. The intersection of the uncertainty value set with the critical line determines the *critical uncertainty value set* $\mathcal{V}_c(\omega) := \mathcal{V}(\omega) \cap r(\omega)$ which may be (i) a single straight-line segment or a single isolated point (in which case $\mathcal{V}_c(\omega)$ is a convex set) or (ii) a union of disjoint straight-line segments and isolated points (in which case $\mathcal{V}_c(\omega)$ is a non-convex set). Figure 2 shows the case of a non-convex critical uncertainty value set. Finally, the boundary of the uncertainty value set is denoted $\partial\mathcal{V}(\omega)$, and the set of *critical boundary-intersections* $\mathcal{B}_c(\omega)$ is defined as

$$\mathcal{B}_c(\omega) := \{\partial\mathcal{V}(\omega) \cap r(\omega)\} \setminus g_0(j\omega)$$

where ' \setminus ' is the set-difference operator. For the special case where $\partial\mathcal{V}(\omega) \cap r(\omega)$ contains $g_0(j\omega)$ as its only element, the following definition is applied:

$$\mathcal{B}_c(\omega) := \{g_0(j\omega)\}$$

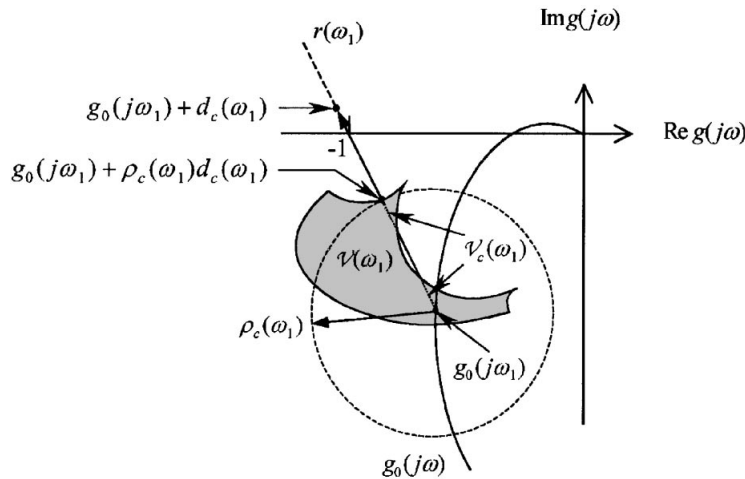


Figure 2. Schematic of an uncertainty value set $\mathcal{V}(\omega_1)$ (shaded area), and the critical perturbation radius $\rho_c(\omega_1)$ at a frequency ω_1 . Also shown in the figure are the critical line $r(\omega_1)$ (dashed line); and the non-convex critical uncertainty value set $\mathcal{V}_c(\omega_1)$ which in this case is the union of two disjoint straight-line segments (shown by the dotted lines).

Note that to determine $\mathcal{B}_c(\omega)$ it is necessary to have knowledge of the uncertainty value set boundary only along the critical line. Clearly, $\mathcal{B}_c(\omega)$ contains a single element if $\mathcal{V}_c(\omega)$ is a convex set, and contains at least two elements if $\mathcal{V}_c(\omega)$ is non-convex.

When the critical value set $\mathcal{V}_c(\omega)$ is convex (as in the case of star-shaped value sets with respect to the nominal point, for example), the *critical perturbation radius* is defined as [1, 2]

$$\rho_c(\omega) := \max_{\alpha \in \mathbb{R}^+} \{ \alpha \mid z = g_0(j\omega) + \alpha d_c(j\omega) \in \mathcal{V}(\omega) \} \tag{2}$$

Definition (2) states that the critical perturbation radius for the case of a convex set $\mathcal{V}_c(\omega)$ is simply the distance along the critical direction between the nominal point $g_0(j\omega)$ and the uncertainty value set boundary $\partial\mathcal{V}(\omega)$. Note also that the critical perturbation radius captures the ‘size’ of the uncertainty that is relevant for stability analysis. Definition (2) is not suitable, however, for the case of non-convex critical value sets $\mathcal{V}_c(\omega)$. In this paper, we propose the following generalization of the definition of the critical perturbation radius, which is applicable to both the convex and non-convex cases:

$$\rho_c(\omega) := \begin{cases} |1 + g_0(j\omega)| - \xi(\omega) & \text{if } -1 + j0 \notin \mathcal{V}(\omega) \\ |1 + g_0(j\omega)| + \xi(\omega) & \text{otherwise} \end{cases} \tag{3}$$

where

$$\xi(\omega) = \min_{z \in \mathcal{B}_c(\omega)} |1 + z| \tag{4}$$

represents the distance from $-1+j0$ to the point in $\mathcal{B}_c(\omega)$ that is closest to the critical point $-1+j0$. The upper statement in definition (3) states that when $-1+j0$ is not an element of $\mathcal{V}(\omega)$, the critical perturbation radius $\rho_c(\omega)$ is defined as the difference between two distances, namely, the distance from the critical point $-1+j0$ to the nominal point $g_0(j\omega)$ (represented by $|1+g_0(j\omega)|$) and the distance from the critical point $-1+j0$ to the closest critical-boundary intersection (represented by $\zeta(\omega)$). On the other hand, when $-1+j0$ is an element of $\mathcal{V}(\omega)$, the lower statement in (3) states that the critical perturbation radius is taken as the sum of the two distances in question. Observe that when the critical uncertainty value set is convex, $\mathcal{B}_c(\omega)$ has only one element (i.e. there is only one critical boundary intersection), and definition (3) becomes equivalent to definition (2). Note also that to compute the critical perturbation radius from (3) it is necessary to have full knowledge of the set of critical boundary intersections $\mathcal{B}_c(\omega)$ and to be able to evaluate whether the set membership condition $-1+j0 \in \mathcal{V}(\omega)$ holds; both of these issues are completely resolved in Sections 3 and 4 of this paper for the case of systems with real affine parametric uncertainties. For either definition it can be shown that $\rho_c(\omega) \geq 0$ for all frequencies. Finally, the *Nyquist robust stability margin*

$$k_N(\omega) := \frac{\rho_c(\omega)}{|1+g_0(j\omega)|} \tag{5}$$

is defined as the ratio of the critical perturbation radius to the distance between the nominal point $g_0(j\omega)$ and the critical point $-1+j0$ measured along the critical direction. Note that $k_N(\omega) \geq 0$ for all frequencies.

2.2. Analysis of Robust Stability

The analysis of the robust stability of the uncertain feedback system being considered can now be given in terms of the following theorem.

Theorem 1

Consider the uncertain system $g(s)$ given in (1) with assumptions (A1) and (A2). Then, the closed-loop system is robustly stable under unity feedback if and only if

$$-1+j0 \notin \mathcal{V}(\omega) \quad \forall \omega \tag{6}$$

Theorem 1 is simply a restatement of the well-known zero-exclusion principle [9], and it gives a necessary and sufficient condition for the robust stability of the closed loop in question. However, Theorem 1 does not provide a measure of the degree of robust stability of the loop, a quantity that would be most useful as the basis for the synthesis of optimally robust controllers or for the assessment of the relative merits of alternative control schemes. The critical direction theory seeks to quantify the robust stability of such systems in terms of the Nyquist robust stability margin (5), which plays a role analogous to that of the structured singular value [3] and of the multivariable stability margin [4]. Efficiency in the analysis is obtained through the realization that it suffices to verify condition (6) only for value-set points that lie along the critical direction; more precisely, the set membership condition (6) holds if and only if $-1+j0 \notin \mathcal{V}_c(\omega)$ holds. These observations lead to the following key result of the critical direction theory.

Theorem 2

Consider the uncertain system $g(s)$ given in (1) with assumptions (A1) and (A2). Then the closed-loop system is robustly stable under unity feedback if and only if

$$k_N(\omega) < 1 \quad \forall \omega \quad (7)$$

Proof

A complete proof is given in Latchman and Crisalle [2] for the case where $\mathcal{V}_c(\omega)$ is convex. For the non-convex case in which the generalized definition (3) of $\rho_c(\omega)$ is utilized the proof is extended as follows. From Theorem 1 the uncertain closed-loop system is stable if and only if $-1 + j0 \notin \mathcal{V}(\omega) \quad \forall \omega$. Therefore, to prove that (7) is sufficient for robust stability, we must show that if $k_N(\omega) < 1 \quad \forall \omega$ then $-1 + j0 \notin \mathcal{V}(\omega) \quad \forall \omega$. To prove by contradiction, assume that $k_N(\omega) < 1 \quad \forall \omega$ and that $\exists \omega$ such that $-1 + j0 \in \mathcal{V}(\omega)$. Then applying definitions (3) and (5) for a frequency at which $-1 + j0 \in \mathcal{V}(\omega)$ gives

$$k_N(\omega) = \frac{\rho_c(\omega)}{|1 + g_0(j\omega)|} = \frac{|1 + g_0(j\omega)| + \xi(\omega)}{|1 + g_0(j\omega)|} = 1 + \frac{\xi(\omega)}{|1 + g_0(j\omega)|}$$

where $\xi(\omega)$ is the non-negative real scalar given by (4). Hence $k_N(\omega) \geq 1$ for at least one frequency, which contradicts the assumption. Therefore, if $k_N(\omega) < 1 \quad \forall \omega$ then it follows that $-1 + j0 \notin \mathcal{V}(\omega) \quad \forall \omega$. To prove that (7) is necessary for robust stability, one must show that if $-1 + j0 \notin \mathcal{V}(\omega) \quad \forall \omega$ then $k_N(\omega) < 1 \quad \forall \omega$. To establish this, note that if $-1 + j0 \notin \mathcal{V}(\omega) \quad \forall \omega$ then by definitions (3) and (5)

$$k_N(\omega) = \frac{\rho_c(\omega)}{|1 + g_0(j\omega)|} = \frac{|1 + g_0(j\omega)| - \xi(\omega)}{|1 + g_0(j\omega)|} = 1 - \frac{\xi(\omega)}{|1 + g_0(j\omega)|} \quad \forall \omega$$

where $\xi(\omega)$ is given by (4). In this case, however, since $-1 + j0 \notin \mathcal{V}(\omega)$ it follows that $-1 + j0 \notin \mathcal{B}_c(\omega)$, and thus $\xi(\omega)$ must necessarily be a positive number. Using this fact in the above equality leads to the conclusion that $k_N(\omega) < 1 \quad \forall \omega$. \square

From Theorem 2 it follows that the scalar $k_N(\omega)$ serves to quantify the robust stability of the closed-loop system. The computation of $k_N(\omega)$ requires knowledge of the critical perturbation radius $\rho_c(\omega)$ defined in (3). The challenging task in a given problem is in fact the calculation of the critical perturbation radius.

When $\mathcal{V}_c(\omega)$ is convex, definition (2) indicates that $\rho_c(\omega)$ represents the distance between the point $g_0(j\omega)$ and the (unique) point where the critical line intersects the boundary of $\mathcal{V}(\omega)$. On the other hand, when $\mathcal{V}_c(\omega)$ is non-convex there are multiple points where the critical line intersects the boundary of $\mathcal{V}(\omega)$. In such cases, definition (3) indicates that $\rho_c(\omega)$ is a function of the distance between $g_0(j\omega)$ and the boundary-intersection point that is closest to the critical point $-1 + j0$. Since in many cases the convexity of $\mathcal{V}_c(\omega)$ at any given frequencies may not be known *a priori*, the generalized critical radius definition allows the application of the critical direction theory without conservatism to a more general class of uncertain systems, including the case of real affine uncertain systems discussed in ensuing sections. The Nyquist robust stability margin $k_N(\omega)$ computed using the general definition (3) for $\rho_c(\omega)$, is attractive from an analysis standpoint because through Theorem 2 it gives necessary and sufficient conditions for robust stability. On the other hand, if $k_N(\omega)$ is computed using equation (2) for $\rho_c(\omega)$, then the

condition $k_N(\omega) < 1 \forall \omega$ is only sufficient for robust stability when the set $\mathcal{V}_c(\omega)$ is non-convex. From a control design point of view, however, it may be advantageous to adopt the computationally simpler definition (2) even for the case where $\mathcal{V}_c(\omega)$ is non-convex, and accept the result as a suboptimal design, as is done in the context of the structured singular value paradigm where control design is based on an upper bound rather than on the exact value of the structured singular value. It must be remarked, however, that when $\mathcal{V}_c(\omega)$ is in fact convex, using definition (2) for $\rho_c(\omega)$ makes the resulting condition $k_N(\omega) < 1 \forall \omega$ necessary and sufficient for robust stability; and in such cases the results are not conservative. It must also be emphasized that the uncertainty value set $\mathcal{V}(\omega)$ itself does not have to be convex for the critical uncertainty value set $\mathcal{V}_c(\omega)$ to be convex.

3. SYSTEMS WITH AFFINE UNCERTAINTY STRUCTURE

In the remaining sections the generalized critical direction theory developed in Section 2 is specialized to systems with real parametric uncertainties that appear in an affine fashion, namely, an uncertain rational function of the form

$$g(s, \mathbf{q}) = \frac{n_0(s) + \sum_{i=1}^p q_i n_i(s)}{d_0(s) + \sum_{i=1}^p q_i d_i(s)}, \quad \mathbf{q} \in Q \tag{8a}$$

where

$$n_0(s) := \sum_{k=0}^{\ell} n_{0k} s^k$$

and

$$d_0(s) := \sum_{k=0}^m d_{0k} s^k$$

are known nominal polynomials,

$$n_i(s) := \sum_{k=0}^{\ell} n_{ik} s^k$$

and

$$d_i(s) := \sum_{k=0}^m d_{ik} s^k$$

are known perturbation polynomials, and $\mathbf{q} = [q_1 \ q_2 \ \dots \ q_p]^T \in R^p$ is a vector of real perturbation parameters belonging to the bounded rectangular polytope

$$Q = \{ \mathbf{q} \in R^p \mid q_i^- \leq q_i \leq q_i^+, \ i = 1, 2, \dots, p \} \tag{8b}$$

where q_i^- and q_i^+ , $i = 1, 2, \dots, p$ are finite real bounds. Equations (8a) and (8b) define a class of finite dimensional, linear, time-invariant, real plants with affine parametric uncertainties. For completeness, the perturbation family Δ is implicitly understood to be the set $\Delta := \{ \delta(s, \mathbf{q}) = g(s, \mathbf{q}) - g(s, \mathbf{q}_0) \mid \mathbf{q} \in Q \}$ for this class of uncertainties.

The value set $\mathcal{V}(\omega)$ at a given frequency ω is defined as the set of the Nyquist-plane points $g(j\omega, \mathbf{q})$ obtained for all $\mathbf{q} \in Q$. Let $\partial\mathcal{V}(\omega)$ represent the boundary of the uncertainty value set $\mathcal{V}(\omega)$ and $E(Q)$ represent the $2^{p-1}p$ edges of the bounding set Q . Furthermore, let $g(j\omega, E(Q))$ represent the *frame* of the value set, namely, the image of the edges of Q on the Nyquist plane under the mapping $g(j\omega, \mathbf{q})$. Two important properties of the value sets generated by systems with affine uncertainty are the following [5]: (i) at each fixed frequency the boundary $\partial\mathcal{V}(\omega)$ of the uncertainty value set $\mathcal{V}(\omega)$ is spanned by the image of the edges of Q , *e.g.* $\partial\mathcal{V}(\omega)$ is spanned by the frame of the value set and (ii) the image of each edge of Q is either a circular arc or a line segment that can be easily calculated analytically. The second property is a consequence of the affine structure of the uncertainty which induces a linear fractional mapping. In the following sections we exploit these properties to develop a computational approach to find the Nyquist stability margin for affine uncertain systems. The results allow the efficient verification of the set membership (6) invoked in Theorem 1 via a linear feasibility problem, and permit the calculation of the robust stability margin invoked in Theorem 2 via a systematic algorithm.

4. ROBUST STABILITY AND UNCERTAINTY VALUE-SET MEMBERSHIP

The first step in the computation of the generalized critical perturbation radius for the uncertain system (8a)–(8b) is to determine whether the critical point $-1 + j0$ belongs to the uncertainty value set $\mathcal{V}(\omega)$. The more general problem of determining if an arbitrary point $w \in C$ belongs to $\mathcal{V}(\omega)$ is solved in this section, and the results are then utilized to reformulate Theorem 1 in terms of computable quantities.

The affine uncertain system (8) can be written in the vector–matrix form

$$g(s, \mathbf{q}) = \frac{[1 \ s \ \dots \ s^{\ell-1} \ s^\ell] \left(\begin{bmatrix} n_{00} \\ n_{01} \\ \vdots \\ n_{0\ell} \end{bmatrix} + \begin{bmatrix} n_{10} & n_{20} & \dots & n_{p0} \\ n_{11} & n_{21} & \dots & n_{p1} \\ \vdots & \vdots & \ddots & \vdots \\ n_{1\ell} & n_{2\ell} & \dots & n_{p\ell} \end{bmatrix} \begin{bmatrix} q_1 \\ q_2 \\ \vdots \\ q_p \end{bmatrix} \right)}{[1 \ s \ \dots \ s^{m-1} \ s^m] \left(\begin{bmatrix} d_{00} \\ d_{01} \\ \vdots \\ d_{0m} \end{bmatrix} + \begin{bmatrix} d_{10} & d_{20} & \dots & d_{p0} \\ d_{11} & d_{21} & \dots & d_{p1} \\ \vdots & \vdots & \ddots & \vdots \\ d_{1m} & d_{2m} & \dots & d_{pm} \end{bmatrix} \begin{bmatrix} q_1 \\ q_2 \\ \vdots \\ q_p \end{bmatrix} \right)} = \frac{\mathbf{s}_n^T(\mathbf{n}_0 + \mathbf{N}_p\mathbf{q})}{\mathbf{s}_d^T(\mathbf{d}_0 + \mathbf{D}_p\mathbf{q})} \quad (9)$$

where s_n and s_d are vectors of lengths $\ell + 1$ and $m + 1$, containing powers of the Laplace variable s , and where $\mathbf{n}_0 \in \mathbf{R}^{\ell+1}$, $\mathbf{d}_0 \in \mathbf{R}^{m+1}$, $\mathbf{N}_p \in \mathbf{R}^{(\ell+1) \times p}$ and $\mathbf{D}_p \in \mathbf{R}^{(m+1) \times p}$ are constant vectors and matrices that represent the structure of the affine parametric uncertainty. The value set at frequency ω is obtained by evaluating (9) at $s = j\omega$ for all $\mathbf{q} \in Q$ to yield

$$g(j\omega, \mathbf{q}) = \frac{\mathbf{s}_{n,R}^T(\mathbf{n}_{0,R} + \mathbf{N}_{p,R}\mathbf{q}) + j\mathbf{s}_{n,I}^T(\mathbf{n}_{0,I} + \mathbf{N}_{p,I}\mathbf{q})}{\mathbf{s}_{d,R}^T(\mathbf{d}_{0,R} + \mathbf{D}_{p,R}\mathbf{q}) + j\mathbf{s}_{d,I}^T(\mathbf{d}_{0,I} + \mathbf{D}_{p,I}\mathbf{q})}, \mathbf{q} \in Q \quad (10)$$

where

$$\mathbf{s}_{n,R}^T = [1 - \omega^2 \ \omega^4 \ -\omega^6 \ \dots] \in \mathbf{R}^{[\ell/2]+1}, \quad \mathbf{s}_{n,I}^T = [\omega - \omega^3 \ \omega^5 \ -\omega^7 \ \dots] \mathbf{0} \in \mathbf{R}^{[(\ell+1)/2]}$$

$$\mathbf{s}_{d,R}^T = [1 - \omega^2 \ \omega^4 \ -\omega^6 \ \dots] \in \mathbf{R}^{[m/2]+1}, \quad \mathbf{s}_{d,I}^T = [\omega - \omega^3 \ \omega^5 \ -\omega^7 \ \dots] \in \mathbf{R}^{[(m+1)/2]}$$

$$\mathbf{n}_{0,R} = \begin{bmatrix} n_{00} \\ n_{02} \\ \vdots \end{bmatrix} \in \mathbf{R}^{[\ell/2]+1}, \quad \mathbf{N}_{p,R} = \begin{bmatrix} n_{10} & n_{20} & \dots & n_{p0} \\ n_{12} & n_{22} & \dots & n_{p2} \\ \vdots & \vdots & \dots & \vdots \end{bmatrix} \in \mathbf{R}^{([\ell/2]+1) \times p}$$

$$\mathbf{n}_{0,I} = \begin{bmatrix} n_{01} \\ n_{03} \\ \vdots \end{bmatrix} \in \mathbf{R}^{[(\ell+1)/2]}, \quad \mathbf{N}_{p,I} = \begin{bmatrix} n_{11} & n_{21} & \dots & n_{p1} \\ n_{13} & n_{23} & \dots & n_{p3} \\ \vdots & \vdots & \dots & \vdots \end{bmatrix} \in \mathbf{R}^{[(\ell+1)/2] \times p}$$

$$\mathbf{d}_{0,R} = \begin{bmatrix} d_{00} \\ d_{02} \\ \vdots \end{bmatrix} \in \mathbf{R}^{[m/2]+1}, \quad \mathbf{D}_{p,R} = \begin{bmatrix} d_{10} & d_{20} & \dots & d_{p0} \\ d_{12} & d_{22} & \dots & d_{p2} \\ \vdots & \vdots & \dots & \vdots \end{bmatrix} \in \mathbf{R}^{([m/2]+1) \times p}$$

and

$$\mathbf{d}_{0,I} = \begin{bmatrix} d_{01} \\ d_{03} \\ \vdots \end{bmatrix} \in \mathbf{R}^{[(m+1)/2]}, \quad \mathbf{D}_{p,I} = \begin{bmatrix} d_{11} & d_{21} & \dots & d_{p1} \\ d_{13} & d_{23} & \dots & d_{p3} \\ \vdots & \vdots & \dots & \vdots \end{bmatrix} \in \mathbf{R}^{[(m+1)/2] \times p}$$

where $\lceil \cdot \rceil$ represents the greatest-integer function.

Now consider an arbitrary Nyquist-plane point $w = w_R + jw_I \in C$ with finite magnitude. Clearly, $w \in \mathcal{V}(\omega)$ if and only if there exists a vector $\mathbf{q} \in \mathbf{Q}$ such that $g(j\omega, \mathbf{q}) = w$. Using (10) this condition is equivalent to finding a vector $\mathbf{q} \in \mathbf{Q}$ that solves the equation

$$\frac{\mathbf{s}_{n,R}^T (\mathbf{n}_{0,R} + \mathbf{N}_{p,R}\mathbf{q}) + j\mathbf{s}_{n,I}^T (\mathbf{n}_{0,I} + \mathbf{N}_{p,I}\mathbf{q})}{\mathbf{s}_{d,R}^T (\mathbf{d}_{0,R} + \mathbf{D}_{p,R}\mathbf{q}) + j\mathbf{s}_{d,I}^T (\mathbf{d}_{0,I} + \mathbf{D}_{p,I}\mathbf{q})} = w_R + jw_I \tag{11}$$

This problem can be characterized as a linear equality problem as shown below.

Theorem 3

Let $w \in C$ be an arbitrary point with finite magnitude on the Nyquist plane. Then $w \in \mathcal{V}(\omega)$ if and only if there exists a feasible solution $\mathbf{q} \in \mathbf{R}^p$ to the linear equality

$$\mathbf{A}(w)\mathbf{q} = \mathbf{b}(w) \tag{12a}$$

subject to the linear-inequality constraint

$$\begin{bmatrix} 1 & 0 & 0 & \cdots & 0 \\ -1 & 0 & 0 & \cdots & 0 \\ 0 & 1 & 0 & \cdots & 0 \\ 0 & -1 & 0 & \cdots & 0 \\ \vdots & \vdots & \vdots & \ddots & \vdots \\ 0 & 0 & 0 & \cdots & 1 \\ 0 & 0 & 0 & \cdots & -1 \end{bmatrix} \mathbf{q} \leq \begin{bmatrix} q_1^+ \\ -q_1^- \\ q_2^+ \\ -q_2^- \\ \vdots \\ q_p^+ \\ -q_p^- \end{bmatrix} \tag{12b}$$

where

$$\mathbf{A}(w) := \begin{bmatrix} \mathbf{s}_{n,R}^T \mathbf{N}_{p,R} - w_R \mathbf{s}_{d,R}^T \mathbf{D}_{p,R} + w_I \mathbf{s}_{d,I}^T \mathbf{D}_{p,I} \\ \mathbf{s}_{n,I}^T \mathbf{N}_{p,I} - w_R \mathbf{s}_{d,I}^T \mathbf{D}_{p,I} - w_I \mathbf{s}_{d,R}^T \mathbf{D}_{p,R} \end{bmatrix} \in \mathbf{R}^{2 \times p} \tag{13}$$

$$\mathbf{b}(w) := \begin{bmatrix} -\mathbf{s}_{n,R}^T \mathbf{n}_{0,R} - w_R \mathbf{s}_{d,R}^T \mathbf{d}_{0,R} - w_I \mathbf{s}_{d,I}^T \mathbf{d}_{0,I} \\ -\mathbf{s}_{n,I}^T \mathbf{n}_{0,I} - w_R \mathbf{s}_{d,I}^T \mathbf{d}_{0,I} + w_I \mathbf{s}_{d,R}^T \mathbf{d}_{0,R} \end{bmatrix} \in \mathbf{R}^2 \tag{14}$$

Proof

A finite point $w \in C$ belongs to $\mathcal{V}(\omega)$ if and only if there exists a vector $\mathbf{q} \in \mathbf{Q}$ that satisfies equation (11). Since the denominator on the left-hand side of (11) is non-zero due to the finite magnitude of w , the equality can be rationalized by multiplication by the denominator, and after isolating the real and imaginary parts leads to the equivalent set of equations

$$\begin{bmatrix} \mathbf{s}_{n,R}^T \mathbf{N}_{p,R} - w_R \mathbf{s}_{d,R}^T \mathbf{D}_{p,R} + w_I \mathbf{s}_{d,I}^T \mathbf{D}_{p,I} \\ \mathbf{s}_{n,I}^T \mathbf{N}_{p,I} - w_R \mathbf{s}_{d,I}^T \mathbf{D}_{p,I} - w_I \mathbf{s}_{d,R}^T \mathbf{D}_{p,R} \end{bmatrix} q = \begin{bmatrix} \mathbf{s}_{n,R}^T \mathbf{n}_{0,R} + w_R \mathbf{s}_{d,R}^T \mathbf{d}_{0,R} - w_I \mathbf{s}_{d,I}^T \mathbf{d}_{0,I} \\ -\mathbf{s}_{n,I}^T \mathbf{n}_{0,I} + w_R \mathbf{s}_{d,I}^T \mathbf{d}_{0,I} + w_I \mathbf{s}_{d,R}^T \mathbf{d}_{0,R} \end{bmatrix}$$

which becomes equality (12a) after the matrix $\mathbf{A}(w)$ and the vector $\mathbf{b}(w)$ are defined as given in (13) and (14), respectively. From (8b), the restriction that $\mathbf{q} \in \mathbf{Q}$ can be described by the linear inequality (12b). Hence, it follows that $w \in C$ is an element of $\mathcal{V}(\omega)$ if and only if there exists a feasible solution to the linear equality/inequality problem (12). \square

Theorem 3 poses the uncertainty value set membership problem as a standard linear equality/inequality feasibility problem whose solution can be found in classical linear programming references (see Reference [12], for example). The linear map given by (12)–(14) is obtained for the rational function (1) with the affine uncertainty structure given by (8). A formally analogous linear map based on the zero-exclusion principle has been developed by Bhattacharyya *et al.* [13] for the case of affine uncertain polynomials. Equations (12)–(14) constitute an extension of that approach to the case of rational systems, and a generalization to the case of an arbitrary point on the complex plane.

To calculate the critical perturbation radius using (3) it is necessary to determine if $-1 + j0$ is an element of the uncertainty value set $\mathcal{V}(\omega)$. From Theorem 1, the solution to this set-membership problem directly defines the robust stability of the system. Therefore, the robust stability of systems with real affine parametric uncertainty can be efficiently determined by

solving the feasibility problem by specializing Theorem 3 to the case $w = -1 + j0$. The result is given in the following theorem.

Theorem 4

Consider the real affine uncertain system given in (6a) and (6b) with assumptions (A1) and (A2). Then the closed-loop system is robustly stable under unity feedback if and only if the following linear equality/inequality problem in $\mathbf{q} \in \mathbf{R}^p$ is infeasible at all frequencies:

$$\mathbf{A}(-1 + j0)\mathbf{q} = \mathbf{b}(-1 + j0) \tag{15a}$$

subject to

$$\begin{bmatrix} 1 & 0 & 0 & \cdots & 0 \\ -1 & 0 & 0 & \cdots & 0 \\ 0 & 1 & 0 & \cdots & 0 \\ 0 & -1 & 0 & \cdots & 0 \\ \vdots & \vdots & \vdots & \ddots & \vdots \\ 0 & 0 & 0 & \cdots & 1 \\ 0 & 0 & 0 & \cdots & -1 \end{bmatrix} \mathbf{q} \leq \begin{bmatrix} q_1^+ \\ -q_1^- \\ q_2^+ \\ -q_2^- \\ \vdots \\ q_p^+ \\ -q_p^- \end{bmatrix} \tag{15b}$$

where

$$\begin{aligned} \mathbf{A}(-1 + j0) &= \begin{bmatrix} -\mathbf{s}_{n,R}^T \mathbf{N}_{p,R} + \mathbf{s}_{d,I}^T \mathbf{R}_{p,R} \\ -\mathbf{s}_{n,I}^T \mathbf{N}_{p,I} + \mathbf{s}_{d,I}^T \mathbf{D}_{p,I} \end{bmatrix} \in \mathbf{R}^{2 \times p} \\ \mathbf{b}(-1 + j0) &= \begin{bmatrix} -\mathbf{s}_{n,R}^T \mathbf{n}_{0,R} - \mathbf{s}_{d,R}^T \mathbf{d}_{0,R} \\ -\mathbf{s}_{n,I}^T \mathbf{n}_{0,I} - \mathbf{s}_{d,I}^T \mathbf{d}_{0,I} \end{bmatrix} \in \mathbf{R}^2 \end{aligned}$$

Proof

From Theorem 1, the condition $-1 + j0 \notin \mathcal{V}(\omega)$ for all frequencies ω is necessary and sufficient for ensuring robust stability. The result follows by applying Theorem 3 to the special case of the point $w = -1 + j0$. □

Theorem 4 represents a systematic method for determining the robust stability of systems with real affine parametric uncertainties.

5. COMPUTATION OF THE CRITICAL PERTURBATION RADIUS

The computation of the Nyquist robust stability margin $k_N(\omega)$ for the affine uncertain system (8) requires that the critical perturbation radius $\rho_c(\omega)$ be calculated first. As indicated by (3) and (4), this in turn requires determining the set $\mathcal{B}_c(\omega)$. Once all the elements of $\mathcal{B}_c(\omega)$ have been identified it is straightforward to calculate $\rho_c(\omega)$ from the applicable formulas. For the case of affine-uncertain systems of the form (8a), the critical boundary-intersections set $\mathcal{B}_c(\omega)$ can be effectively identified using a two-step strategy.

The first step consists of finding the set of points $F = \{P_i, i = 1, 2, \dots, k\}$ that correspond to all the intersections between the critical line $r(\omega)$ with the frame $g(j\omega, E(Q))$. This reduces to a simple problem in two-dimensional computational geometry after recognizing that the critical line is a ray and that the frame is a collection of arcs of circles and straight-line segments. Further details are given in Section 5.1. Note that all the points in the frame-intersection set F are elements of $\mathcal{V}_c(\omega)$ because each point in turn belongs to $r(\omega)$. It is straightforward to conclude that $\mathcal{B}_c(\omega) \subseteq F$ after arguing that some elements of the frame-intersection set F may not lie on the value-set boundary $\partial\mathcal{V}(\omega)$, and that all elements of $\mathcal{B}_c(\omega)$ must be elements of F .

The second step consists of constructing the set of critical intersections $\mathcal{B}_c(\omega)$ by selecting from F all the points that also belong to $\mathcal{B}_c(\omega)$. For the special case where $F = \{g_0(j\omega)\}$ it follows that $\mathcal{B}_c(\omega) = \{g_0(j\omega)\}$. For the more general case where $g_0(j\omega)$ is not the only element of F , then $\mathcal{B}_c(\omega)$ is constructed by selecting all the points in F that lie on the boundary $\partial\mathcal{V}(\omega)$. In accordance with the general definition of $\mathcal{B}_c(\omega)$, the point $g_0(j\omega)$ must be excluded. Therefore, if $g_0(j\omega) \in F$, the set F must be redefined by excluding from it the element $g_0(j\omega)$ through the assignment $F \setminus g_0(j\omega) \rightarrow F$. Without loss of generality, assume that the points in F are ordered in increasing distance from the nominal point $g_0(j\omega)$, and that P_1 and P_k are respectively the closest and farthest points from $g_0(j\omega)$. Clearly, $\mathcal{B}_c(\omega)$ contains the point P_k . When $k > 1$ the additional elements of $\mathcal{B}_c(\omega)$ can be readily identified from F by considering all the straight-line segments $P_n P_{n+1}, n = 1, 2, \dots, k - 1, P_n \in F$. Clearly, if one interior point of the segment $P_n P_{n+1}$ lies outside the value set $\mathcal{V}(\omega)$, it can be concluded that both P_n and P_{n+1} lie on the boundary of the value set and hence, both P_n and P_{n+1} are elements of $\mathcal{B}_c(\omega)$. It is easily seen that this is a necessary and sufficient condition for the membership of P_n and P_{n+1} in $\mathcal{B}_c(\omega)$. All the elements of $\mathcal{B}_c(\omega)$ can be systematically identified through such a sequential analysis of the points in F . Note that to determine if the end points of a given segment $P_n P_{n+1}$ belong to $\mathcal{B}_c(\omega)$ it suffices to test if any interior point, say the midpoint, of the segment lies outside of $\mathcal{V}_c(\omega)$. This set membership condition can be readily determined by applying Theorem 3 to the segment midpoint.

5.1. Intersection of a ray and arcs in the complex plane

As discussed above, the first step in the computation of the critical perturbation radius consists of finding the set of points $F = \{P_i(\omega), i = 1, 2, \dots, k\}$ that correspond to intersections of the critical line $r(\omega)$ with the frame $g(j\omega, E(Q))$. This is equivalent to determining the intersection of a ray (the critical line) and arcs or straight-line segments (the frame) in the complex plane. The equations needed for characterizing the intersection of the critical line with straight-line segments are trivial and are therefore omitted for brevity. The determination of all the intersections of the critical line with a finite number κ of arcs of circle is somewhat more subtle and is therefore discussed in greater detail.

The basic geometric objects of interest are defined as follows. A line passing through two points $p_0, p_1 \in C$ can be represented by

$$L(p_0, p_1) := \{z \in C \mid z = p_0 + t(p_1 - p_0), t \in R\} \quad (16)$$

The same relation can be used to represent a ray, $r(p_0, p_1)$ with origin at p_0 and pointing towards p_1 by restricting the parameter t to adopt only non-negative values. The line $L(p_0, p_1)$ is said to be the supporting line for $r(p_0, p_1)$. The critical direction $r(\omega)$ is therefore represented by the ray $r(p_0, p_1)$ with $p_0 = g_0(j\omega)$ and $p_1 = -1 + j0$.

Consider a set κ of circles with center at points $z_i \in C$ and radii $r_i \in R, i = 1, 2, \dots, \kappa$, where each circle satisfies the relation

$$C_i := \{z \in C \mid (\overline{z - z_i})(z - z_i) = r_i^2, r_i > 0\} \tag{17}$$

Therefore, two parameters are sufficient to define each circle. On the other hand, three parameters are required to describe an oriented circular arc that passes through three points $a_0, a_1, a_2 \in C$, in that order, and such an arc will be denoted implicitly as $a_i(a_0, a_1, a_2)$ if it belongs to a supporting circle C_i .

The relative position of a set of points and orientation of arcs and rays in the plane can easily be determined invoking the cross product operation. Let $p_0, p_1 \in C$, then the cross product of p_0 and p_1 can be defined as

$$p_0 \times p_1 := \text{Im}\{\bar{p}_0 p_1\}$$

The sign of the cross product determines the relative orientation of p_0 and p_1 with respect to the origin: p_1 lies to left (right) of p_0 if $p_0 \times p_1 < 0$ (> 0), and p_1 and p_0 are collinear if $p_0 \times p_1 = 0$ [14]. The cross product can also be used to determine the direction in which an oriented circular arc ‘turns’. Let $a(a_0, a_1, a_2)$ be a circular arc that originates at a_0 , passes through a_1 , and ends at a_2 . Then, the arc turns left (right) if $(a_2 - a_0) \times (a_1 - a_0) > 0$ (< 0). If $(a_2 - a_0) \times (a_1 - a_0) = 0$ the three points are collinear, and the arc degenerates into a line segment. The arc $a(a_0, a_1, a_2)$ is said to be positive (negative) if it turns left (right).

The following four-step strategy to compute the intersection of a ray and a finite number of arcs is proposed: (i) find $I^{(i)} = L(g_0(j\omega, -1 + j0)) \cap C_i$, the set of the intersections (if any) of the supporting line (i.e. the line that contains the critical ray) and the i th supporting circle (i.e. the circle that contains the i th arc); (ii) find $I_r^{(i)} = r(g_0(j\omega, -1 + j0)) \cap I^{(i)}$, the set of intersections of the critical ray and the supporting circle; (iii) find $I_{ar}^{(i)} = a_i \cap I_r^{(i)} \subset I_r^{(i)}$, the intersections of the critical ray and the i th arc and (iv) find $F = \cup_{1 \leq i \leq \kappa} I_{ar}^{(i)}$, the union over all arcs of all the possible ray–arc intersections. The set F corresponds to the desired set of intersections of the critical line $r(\omega)$ with the elements of the frame of $g(j\omega, E(Q))$ that are described by arcs of circles. The remaining elements of the set F are of course the set of points that represent the intersections of $r(\omega)$ with the elements of the frame of $g(j\omega, E(Q))$ that are described by straight-line segments.

Each of the four steps outlined above can be quantified in more precise terms. To execute step (i), consider a ray $r(p_0, p_1)$ and an oriented arc $a_i(a_0, a_1, a_2)$ whose respective supporting line $L(p_0, p_1)$ and supporting circle C_i are given by (16) and (17). The set of intersections $I^{(i)}$ of the supporting line and supporting circle is determined by the real solutions of the quadratic equation $at^2 + bt + c = 0$, where $a = |p_1 - p_0|^2$, $b = 2 \text{Re}\{(\overline{p_1 - p_0})(p_1 - z_i)\}$, and $c = |p_0|^2 + |z_i|^2 - (r_i^2 + 2 \text{Re}\{\overline{p_0 z_i}\})$. It readily follows that there are no intersections if the discriminant $d := b^2 - 4ac$ is negative. Furthermore, if the discriminant is zero the supporting line is tangential to the circle and there is only one intersection. Finally, there are two intersections if the discriminant is positive. Now let $\{t_1, t_2\}$, denote the one or two real solutions to the quadratic equation for the case where the discriminant is non-negative. The set of intersection points $I^{(i)}$ is composed of the points z in Equation (16) obtained by setting $t = t_k, k = 1, 2$. To execute step (ii) and find $I_r^{(i)} \subset I^{(i)}$ it is sufficient to discard the points of $I^{(i)}$ that correspond to negative values of t_k . To complete step (iii), the set $I_{ar}^{(i)} \subset I_r^{(i)}$ can be determined using the cross product properties. Consider an arc $a_i(a_0, a_1, a_2)$ and an intersection point $y \in I_r^{(i)}$. Then y belongs to $I_{ar}^{(i)}$ if and only if the arcs $a_i(a_0, a_1, a_2)$ and $a_i(a_0, y, a_2)$ are both positive or both

negative (i.e. both arcs turn in the same direction). Finally, step (iv) is completed by setting the set F as the union of the sets $I_{ar}^{(i)}$ obtained when considering all the arcs $C_i, i = 1, 2, \dots, \kappa$.

6. EXAMPLES

Consider the system with affine uncertainty structure

$$g(s, \mathbf{q}) = \frac{(0.3s^3 + 2.2s^2 + 10s + 20) + (0.12s^2 + 0.7s + 1)q_1 + (0.06s^2 + 0.2s)q_2 + (-0.3s - 1)q_3}{(s^4 + 9.5s^3 + 27s^2 + 22.5s + 0.1) + (0.5s^3 + 2s^2 - s)q_1 + (0.5s^3 + s^2)q_2 + (-0.5s^3 + s)q_3} \tag{18}$$

where the parameter vector $\mathbf{q} = [q_1 \ q_2 \ q_3]^T$ is an element of a rectangular polytope $\mathbf{Q} \subset \mathbf{R}^3$, and where the nominal system $g_0(s) = g(s, \mathbf{q}_0)$ is obtained with $\mathbf{q}_0^T = [0 \ 0 \ 0]$. System (18) is a modified version of the model investigated by Fu [5]. The objective is to analyse the robustness of the unity-feedback structure shown in Figure 1. Two examples are given, namely, a case where the critical uncertainty value set is convex and one where the value set is nonconvex.

6.1. Example of a convex critical value set

Consider system (18) where the parametric uncertainty vector belongs to the square polytope

$$Q = \{\mathbf{q} \in \mathbf{R}^3 \mid -3 \leq q_i \leq 3, i = 1, 2, 3\} \tag{19}$$

Figure 3 shows the frame $g(j\omega, \mathbf{E}(Q))$ of the uncertainty value set at the frequency $\omega = 0.7$. At this frequency it is readily concluded by inspection that the critical value set $\mathcal{V}_c(\omega)$ is convex, since it consists of a single line segment. Note that, in contrast, the entire value set $\mathcal{V}(\omega)$ is nonconvex.

In order to apply Theorem 4, consider the frequency $\omega = 0.7$ and define the following elements:

$$\mathbf{s}_{n,R}^T = [1.000 \quad -0.4900], \quad \mathbf{s}_{n,I}^T = [0.7000 \quad -0.3430] \tag{20a}$$

$$\mathbf{s}_{d,R}^T = [1.0000 \quad -0.4900 \quad 0.2401], \quad \mathbf{s}_{d,I}^T = [0.7000 \quad -0.3430] \tag{20b}$$

$$\mathbf{n}_{0,R} = \begin{bmatrix} 20 \\ 2.2 \end{bmatrix}, \quad \mathbf{N}_{p,R} = \begin{bmatrix} 1 & 0 & -1 \\ 0.12 & 0.06 & 0 \end{bmatrix} \tag{20c}$$

$$\mathbf{n}_{0,I} = \begin{bmatrix} 10 \\ 0.3 \end{bmatrix}, \quad \mathbf{N}_{p,I} = \begin{bmatrix} 0.7 & 0.2 & -0.3 \\ 0 & 0 & 0 \end{bmatrix} \tag{20d}$$

$$\mathbf{d}_{0,R} = \begin{bmatrix} 0.1 \\ 27 \\ 1 \end{bmatrix}, \quad \mathbf{D}_{p,R} = \begin{bmatrix} 0 & 0 & 0 \\ 2 & 1 & 0 \\ 0 & 0 & 0 \end{bmatrix} \tag{20e}$$

$$\mathbf{d}_{0,I} = \begin{bmatrix} 22.5 \\ 9.5 \end{bmatrix}, \quad \mathbf{D}_{p,I} = \begin{bmatrix} -1 & 0 & 1 \\ 0.5 & -0.5 & 0.5 \end{bmatrix} \tag{20f}$$

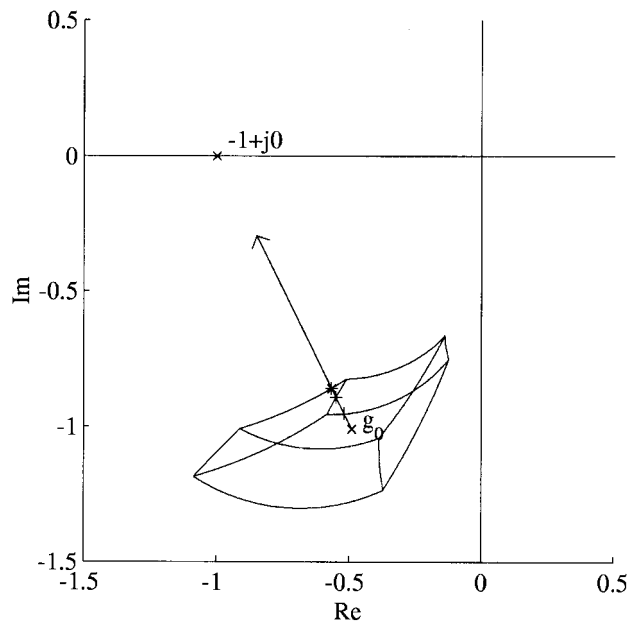


Figure 3. Frame of the uncertainty value set for the system of Example 6.1 at the frequency $\omega = 0.7$. The critical point $-1 + j0$ and the nominal point $g_0(j\omega)$ are represented by the 'x' markers, the three intersections of the arcs with the critical line are represented by the '+' markers, and the intersection that defines the boundary point used in the calculation of $\rho_c(\omega)$ is represented by the '*' marker. The critical value set $\mathcal{V}_c(\omega)$ is convex at this frequency, as it is represented by a single straight-line segment.

and

$$\mathbf{A}(-1 + j0) = \begin{bmatrix} 1.1572 & -0.4527 & -1.4624 \\ -0.8534 & -0.1930 & -0.0848 \end{bmatrix} \tag{21}$$

$$\mathbf{b}(-1 + j0) = \begin{bmatrix} -0.8049 \\ -2.5870 \end{bmatrix} \tag{22}$$

For this problem, the constraint (15b) is

$$\begin{bmatrix} 1 & 0 & 0 \\ -1 & 0 & 0 \\ 0 & 1 & 0 \\ 0 & -1 & 0 \\ 0 & 0 & 1 \\ 0 & 0 & -1 \end{bmatrix} \mathbf{q} \leq \begin{bmatrix} 3 \\ 3 \\ 3 \\ 3 \\ 3 \\ 3 \end{bmatrix} \tag{23}$$

It can be readily verified using an active-set method [12] that the linear equality/inequality problem (15a)–(15b) with the data shown above is infeasible. Invoking Theorem 4 it then

follows that $-1 + j0 \notin \mathcal{V}(\omega)$ and hence it can be claimed that at $\omega = 0.7$ the value set $\mathcal{V}(\omega)$ excludes the critical point.

In order to quantify the degree of robust stability at this frequency, it is useful to calculate the value of the Nyquist robust stability margin. It is possible to calculate $\rho_c(\omega)$ following the procedure discussed in Section 5. The first step consists of finding the set of points $F = \{P_i, i = 1, 2, \dots, k\}$ that define all the intersections of the critical line $r(\omega)$ with the frame $g(j\omega, \mathbf{E}(Q))$. It follows that $F = \{-0.5185 - j0.9523, -0.5494 - j0.8913, -0.5660 - j0.8584\}$. The elements of $\mathcal{B}_c(\omega)$ can be found using the systematic procedure discussed in Section 5; however, it is also possible to identify the set from Figure 3, where it is clear that only one element of F , namely $-0.5660 - j0.8584$, lies on the boundary; therefore $\mathcal{B}_c(\omega) = \{-0.5660 - j0.8584\}$. As expected, $\mathcal{B}_c(\omega)$ contains only one element because $\mathcal{V}_c(\omega)$ is convex. Next, using definition (3) one finds that at $\omega = 0.7$ the critical perturbation radius is $\rho_c(\omega) = 0.1694$. Furthermore, since at this frequency $g_0(j\omega) = -0.4896 - j1.0096$, it follows that $k_N(\omega) = 0.1694 / |1 - 0.4896 - j1.0096| = 0.1498 < 1$, which is consistent with the claim that at $\omega = 0.7$ the value set excludes the critical point.

Figures 4 and 5, respectively, show the values of $\rho_c(\omega)$ and $k_N(\omega)$ calculated for a grid of 100 non-negative frequency points that are equally spaced in a logarithmic scale in the range $[0.001, 10]$. From Figure 5 it is readily concluded that $k_N(\omega) < 1$ for all the frequencies investigated, and it can then be concluded from Theorem 2 that the closed-loop system is robustly stable.

6.2. Example of a non-convex critical value set

Now reconsider system (18) for the case where the parametric uncertainty vector belongs to the rectangular polytope

$$Q = \{\mathbf{q} \in R^3 \mid -10 \leq q_1 \leq 10, -0.3 \leq q_2 \leq 0.3, -0.3 \leq q_3 \leq 0.3\} \tag{24}$$

With this modification to the example discussed in Section 6.1 the system now has a non-convex critical uncertainty value set $\mathcal{V}_c(\omega)$ at the frequency $\omega = 0.95$, as can be determined by inspection of the frame $g(j\omega, E(Q))$ of the value set shown in Figure 6. The figure clearly shows that, as one follows the critical-direction ray from the nominal point $g_0(j\omega)$ to the critical point, the ray realizes three intersections with the value set boundary. The ray leaves the value set

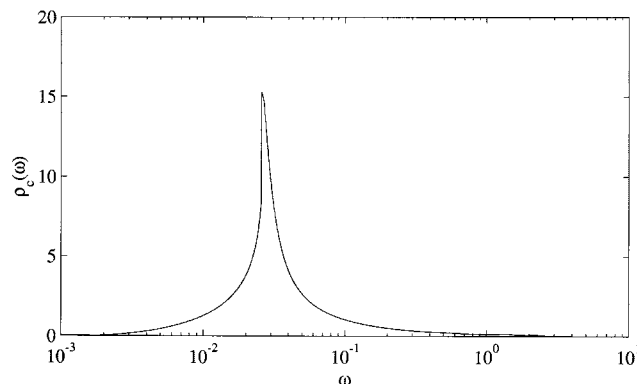


Figure 4. Critical perturbation radius $\rho_c(\omega)$ for the system considered in Example 6.1.

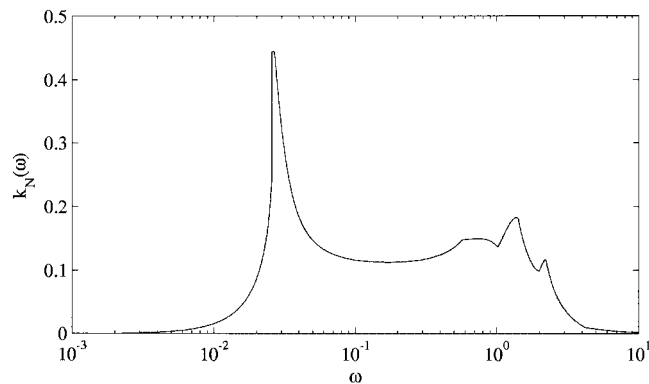


Figure 5. Nyquist robust stability margin $k_N(\omega)$ for the system considered in Example 6.1.

immediately after the first intersection with the boundary occurs, and it does not reenter the value set until it realizes the second intersection with the boundary. As a consequence of this geometry, the critical uncertainty value set $\mathcal{V}_c(\omega)$ is the union of two disjoint line segments, and therefore $\mathcal{V}_c(\omega)$ is non-convex.

When applying Theorem 4 to this system for a particular frequency, the only modification to the feasibility problem presented for the previous example concerns the form of the inequality constraints (15b) which now adopt the form

$$\begin{bmatrix} 1 & 0 & 0 \\ -1 & 0 & 0 \\ 0 & 1 & 0 \\ 0 & -1 & 0 \\ 0 & 0 & 1 \\ 0 & 0 & -1 \end{bmatrix} \mathbf{q} \leq \begin{bmatrix} 10 \\ 10 \\ 0.3 \\ 0.3 \\ 0.3 \\ 0.3 \end{bmatrix} \tag{25}$$

instead of the form (23). The vector and matrix definitions (20a)–(20f) remain unchanged. As in the previous example, it can be readily verified using an active-set method that the linear equality/inequality problem (15a)–(15b) with the data corresponding to this example is infeasible. Invoking Theorem 4, it then follows that $-1 + j0 \notin \mathcal{V}(\omega)$, and hence it can be claimed that at $\omega = 0.95$, the value set excludes the critical point.

The Nyquist robust stability margin $k_N(\omega)$ and the critical perturbation radius $\rho_c(\omega)$ can now be calculated at any frequency using the method described in Section 5. At the frequency $\omega = 0.95$, the set of intersections of the critical line $r(\omega)$ with the frame $g(j\omega, E(Q))$ is

$$F = \{-0.6510 - j0.3738, -0.4196 - j0.6217, 0.6349 - j0.3911, -0.4403 - j0.5995, -0.6512 - j0.3736, -0.6498 - j0.3751\}$$

The elements of $\mathcal{B}_c(\omega)$ can be identified from F using the sequential method described in Section 5 to yield

$$\mathcal{B}_c(\omega) = \{-0.6510 - j0.3738, -0.6349 - j0.3911, -0.6512 - j0.3736\}$$

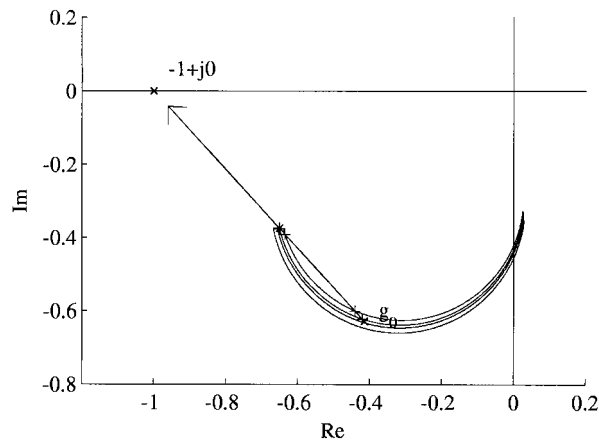


Figure 6. Frame for the uncertainty value set for the system of Example 6.2 at the frequency $\omega = 0.9500$. The critical point $-1 + j0$ and the nominal point $g_0(j\omega)$ are represented by the 'x' markers, the intersections of the arcs with the critical line are represented by the '+' markers, and the intersection that defines the boundary point used in the calculation of $\rho_c(\omega)$ is represented by the '*' marker. The critical value set $\mathcal{V}_c(\omega)$ is nonconvex at this frequency, and it is represented by the union of two disjoint straight-line segments.

which contains three elements due to the non-convexity of $\mathcal{V}_c(\omega)$. Using Equation (4) yields

$$\zeta(\omega) = \min_{z \in \mathcal{B}_c(\omega)} |1 + z| = |1 - 0.6512 - j0.3736| = 0.5111$$

and then invoking definition (3) it is readily determined that

$$\rho_c(\omega) = |1 - 0.4140 - 0.6277j| - 0.5111 = 0.3475$$

at the frequency $\omega = 0.95$. Furthermore, since $g_0(j\omega) = -0.4140 - j0.6277$ at this frequency, it follows that $k_N(\omega) = 0.3475/|1 - 0.4140 - 0.6277j| = 0.4047 < 1$, a result that is consistent with the conclusion reached by invoking Theorem 4 that the value set does not include the critical point at this frequency.

Figures 7 and 8, respectively, show the values of $\rho_c(\omega)$ and $k_N(\omega)$ calculated for a sequence of 250 frequency points equally spaced in a logarithmic scale in the range $[0.001, 10]$. From Figure 8 it is readily concluded that $k_N(\omega) < 1$. Therefore, the feedback loop is robustly stable. Also notice from Figures 7 and 8 that $\rho_c(\omega)$ and $k_N(\omega)$ are discontinuous at frequencies approximately equal to $\omega = 0.020$ and 0.9417 . The presence of such discontinuities is not surprising since it is well known that other stability margins (such as the real- μ robust stability margin) have also shown discontinuities. The observed discontinuities can be explained by examining Figure 6, which shows the frame of a value set at the frequency $\omega = 0.9500$. At this frequency the critical line intersects the boundary of the uncertainty value set at three points (one point near the nominal point and two points closer to $-1 + j0$). The critical uncertainty value set $\mathcal{V}_c(\omega)$ is composed of two disjoint line segments: one segment joining the nominal point with its nearest boundary point, and a second segment joining the other two boundary points. The numerical value of $\rho_c(\omega)$ is in this case calculated using the boundary point closest to $-1 + j0$. As the frequency decreases the uncertainty value set rotates in a counterclockwise

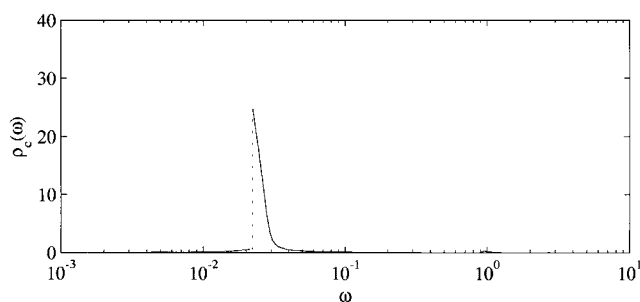


Figure 7. Critical perturbation radius $\rho_c(\omega)$ for the system considered in Example 6.2. An observed discontinuity is shown with a dashed line; a second discontinuity is not visible in the plot due to the tight scale of the ordinate.

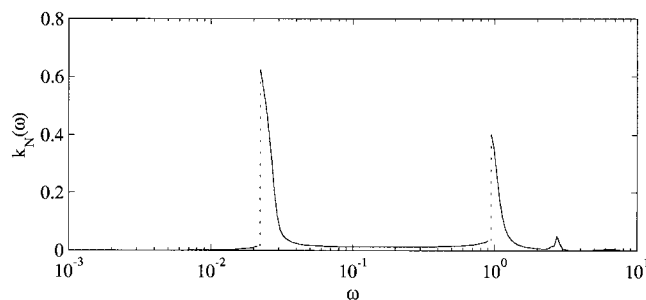


Figure 8. Nyquist robust stability margin $k_N(\omega)$ for the system considered in Example 6.2. Observed discontinuities are shown with a dashed line.

direction. This causes a progressive reduction in the length of the line segment formed by the two boundary points that are closest to $-1 + j0$. Eventually, this line segment collapses into a single point in such a way that the critical line passing through the point is locally tangential to the uncertainty value set. When this situation arises, the critical value set $\mathcal{V}_c(\omega)$ is composed of the tangent point just mentioned and one line segment (namely, that joining the nominal point with its nearest boundary point). This effect is realized at a frequency slightly higher than $\omega = 0.9417$ for the example under consideration, and the value of $\rho_c(\omega)$ must be calculated using the tangent point. As the frequency is reduced slightly below the value $\omega = 0.9417$ the critical line is no longer tangent to the template, and its intersection with the value set defines a single continuous segment, hence, $\mathcal{V}_c(\omega)$ recovers its convexity. The calculation of $\rho_c(\omega)$ is now made using the only existing boundary point, which is now located closer to the nominal point. Hence, as this local decrease in frequency in the neighborhood of $\omega = 0.9417$ requires that the boundary point selected for the calculation of $\rho_c(\omega)$ be changed from the tangent point (located closer to $-1 + j0$) to a non-neighboring point that is located closer to the nominal point; this explains the discontinuity $\rho_c(\omega)$ which in turn causes $k_N(\omega)$ to be discontinuous.

7. CONCLUSIONS

The main contribution of this paper is the generalization of the critical direction theory proposed to analyse the robust stability of systems whose critical uncertainty value sets are non-convex. The generalization is obtained by introducing a new definition of the critical perturbation radius, and the effectiveness of the generalized theory is validated by its success in assigning a quantitative robust stability measure, namely, a computable Nyquist robust stability margin, to problems that involve affine parametric uncertainties characterized by real vectors that belong to a rectangular polytope. For the case considered, the calculation of the Nyquist robust stability margin involves planar geometry operations and solving a series of linear equality/inequality feasibility problems that do not pose major computational challenges.

ACKNOWLEDGEMENTS

The first and last authors gratefully acknowledge support received from the National Science Foundation under grant number CTS 9502936.

REFERENCES

1. Latchman HA, Crisalle OD. Exact robustness analysis for highly structured frequency-domain uncertainties. *Proceedings of the American Control Conference*, Seattle, WA, 1995; 3982–3987.
2. Latchman HA, Crisalle OD, Basker VR. The Nyquist robust stability margin—a new metric for robust stability, *International Journal of Robust and Nonlinear Control* 1997; 7:211–226.
3. Doyle J. Analysis of feedback systems with structured uncertainties. *IEE Proceedings Part D* 1982; 129:242–250.
4. Safonov MG. Stability margins of diagonally perturbed multivariable feedback systems. *IEE Proceedings Part D* 1982; 129:251–256.
5. Fu M. Computing the frequency response of linear systems with parametric perturbations. *Systems and Control Letters* 1990; 15:45–52.
6. Kharitonov VL. Asymptotic stability of an equilibrium position of a family of systems of linear differential equations. *Differentsial'nye Uravneniya* 1978; 14:2086–2088.
7. Kharitonov VL. Asymptotic stability of an equilibrium position of a family of systems of linear differential equations. *Differential Equations* 1979; 14:1483–1485.
8. Chapellat H, Bhattacharyya SP. A generalization of Kharitonov's theorem: robust stability of interval plants, *IEEE Transactions on Automatic Control* 1989; 34:1100–1108.
9. Barmish BR. *New Tools for Robustness of Linear Systems*. McMillan: New York, 1994.
10. Bartlett AC, Tesi A, Vicino A. Frequency response of uncertain systems with interval plants. *IEEE Transactions on Automatic Control* 1990; 38:929–933.
11. Barmish BR. Extreme point results for robust stabilization of interval plants with first order compensators. *IEEE Transactions on Automatic Control* 1992; 37:707–715.
12. Luenberger DG. *Linear and Nonlinear Programming*. Addition-Wesley: Reading, MA, 1984.
13. Bhattacharyya SP, Chapellat H, Keel LH. *Robust Control—The Parametric Approach*. Prentice-Hall: Englewood Cliffs, NJ, 1995.
14. Cormen T, Leiserson C, Rivest R. *Introduction to Algorithms*. McGraw-Hill: New York, 1990.
15. MacFarlane AGJ. *Complex Variable Methods for Linear Multivariable Feedback Systems*. Taylor & Francis: London, 1982.